

Accepted Manuscript

Title: Variability of particle configurations achievable by 2-nozzle flame syntheses of the Au-Pd-TiO₂ system and their catalytic behaviors in the selective hydrogenation of acetylene

Authors: Boontida Pongthawornsakun, Okorn Mekasuwandumrong, Francisco J. Cadete Santos Aires, Robert Büchel, Alfons Baiker, Sotiris E. Pratsinis, Joongjai Panpranot



PII: S0926-860X(17)30443-X
DOI: <http://dx.doi.org/10.1016/j.apcata.2017.09.014>
Reference: APCATA 16408

To appear in: *Applied Catalysis A: General*

Received date: 16-7-2017
Revised date: 10-9-2017
Accepted date: 11-9-2017

Please cite this article as: {<http://dx.doi.org/>

This is a PDF file of an unedited manuscript that has been accepted for publication. As a service to our customers we are providing this early version of the manuscript. The manuscript will undergo copyediting, typesetting, and review of the resulting proof before it is published in its final form. Please note that during the production process errors may be discovered which could affect the content, and all legal disclaimers that apply to the journal pertain.

Variability of particle configurations achievable by 2-nozzle flame syntheses of the Au-Pd-TiO₂ system and their catalytic behaviors in the selective hydrogenation of acetylene

Boontida Pongthawornsakun^a, Okorn Mekasuwandumrong^b, Francisco J. Cadete Santos Aires^c, Robert Büchel^d, Alfons Baiker^e, Sotiris E. Pratsinis^{d}, and Joongjai Panpranot^{a**}*

^aCenter of Excellence on Catalysis and Catalytic Reaction Engineering, Department of Chemical Engineering, Faculty of Engineering, Chulalongkorn University, Bangkok 10330, Thailand

^bDepartment of Chemical Engineering, Faculty of Engineering and Industrial Technology, Silpakorn University, Nakorn Pathom 73000, Thailand

^cInstitut de Recherches sur la Catalyse et l'Environnement de Lyon – IRCELYON (UMR 5256 CNRS/Univ. Lyon I), 2 Avenue Albert Einstein, 69626 – Villeurbanne cedex, France

^dParticle Technology Laboratory, Department of Mechanical and Process Engineering, ETH Zurich, Sonneggstrasse 3, CH-8092 Zurich, Switzerland

^eInstitute of Chemical and Bioengineering, Department of Chemistry and Applied Biosciences, ETH Zurich, Hönggerberg, HCI, CH-8093 Zurich, Switzerland

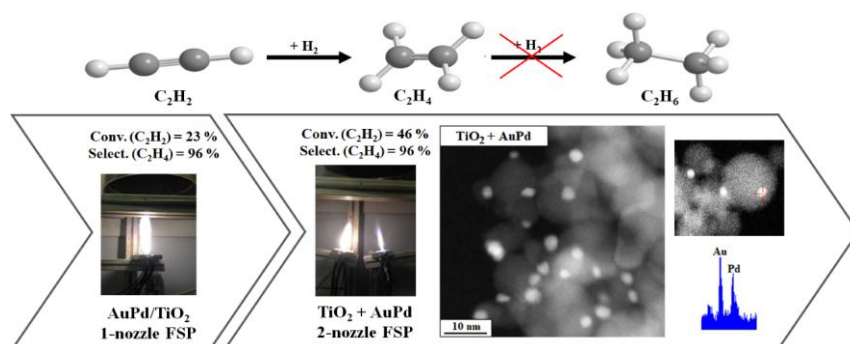
Date: September 10, 2017

Submitted to: *Applied Catalysis A: General*

*,** Corresponding authors.

Tel. 66-2218-6869 Fax. 66-2218-6877 E-mail: joongjai.p@chula.ac.th (J. Panpranot)
sotiris.pratsinis@ptl.mavt.ethz.ch (S. E. Pratsinis)

Graphical abstract



Highlights

- Au-Pd-TiO₂ system with various particle configurations were synthesized by 2-nozzle FSP for the first time.
- Particle compositions, the interaction between metal-metal and metal-support, and the location of Pd (or AuPd) on the TiO₂ were varied.
- Fraction of bimetallic alloy particles on TiO₂ was maximized by feeding Au and Pd precursors to the same nozzle and the Ti precursor to the other one.
- The enhanced hydrogenation activity and high selectivity to ethylene (>95%) is attributed to the presence of bimetallic AuPd alloy particles.

Abstract

Catalysts with Au and Pd supported on TiO₂ (Au:Pd 1:1 wt/wt%) were prepared by 1- and 2-nozzle flame spray pyrolysis (FSP). The 2-nozzle configuration allowed to synthesize various particle configurations by separate or co-feeding of the metal precursor solutions to the two nozzles. For the Au-Pd/TiO₂ system, four different catalyst particle configurations were investigated: "TiO₂ + AuPd", "Pd/TiO₂+Au", "Au/TiO₂+Pd", and "Pd/TiO₂+Au/TiO₂", where + separates the corresponding precursor solutions fed to the two nozzles. There were no significant differences in the specific surface areas and the average TiO₂ crystallite sizes of the catalysts (100 m²/g and 16-17 nm, respectively) with the exception of "Pd/TiO₂

+Au/TiO₂", which exhibited larger surface area and smaller crystallite size (152 m²/g, 12 nm) due to halving of the Ti precursor concentration in each nozzle. As revealed by CO chemisorption, XPS, and STEM-EDX results, the catalyst properties varied largely in terms of bimetallic AuPd particle compositions, the interaction between metal-metal and metal-support, and the location of Pd (or AuPd) on the TiO₂. Among the catalysts studied, "TiO₂+AuPd" prepared with the 2-nozzle system exhibited the highest conversion of acetylene (~50%) at 40°C with high selectivity to ethylene (>95%). Co-feeding the noble metal precursors together with the Ti precursor afforded less active catalysts due to the formation of Ti-O species partially covering the most active bimetallic AuPd particles. Compared to the commercially available acetylene hydrogenation catalyst and the AuPd/TiO₂ prepared by conventional co-impregnation and deposition-precipitation, all the FSP-AuPd/TiO₂ catalysts showed superior performances under the reaction conditions used.

Keywords: flame spray pyrolysis; AuPd/TiO₂; bimetallic AuPd alloy particles; 2-nozzle system; acetylene hydrogenation

1. Introduction

During ethylene polymerization, the feed stream from thermal and/or steam cracking contains small quantities of acetylene (< 2-3%) that poison the polymerization catalysts [1-3]. As a result, polyethylene products may not be properly vulcanized and become brittle [4]. In addition, acetylene can form metal acetylides, which are explosive contaminants [5]. Thus, the acetylene in ethylene feed should be eliminated or reduced to an acceptable level (<5 ppm) [4, 6]. The most commonly used method for acetylene removal is the selective hydrogenation of acetylene using Al₂O₃ supported Pd-based catalysts [7-10]. However, at high acetylene conversion (100%), the catalysts show low ethylene selectivity (11%) [11]. An over-hydrogenation of ethylene to ethane can occur due to the strong adsorption of both reactants and products on the Pd sites [12]. One of the attractive techniques to control the

contact of Pd with reactants and products is the addition of a second metal to form bimetallic catalysts. Gold has been used as such metal for the selective hydrogenation of acetylene [3, 12-15].

The performance of AuPd catalysts in the selective acetylene hydrogenation was found to depend largely on the AuPd structure. For examples, Sárkány et al. [14] reported an activity decrease with increasing of Pd shell thickness of the Pd_{shell}-Au_{core}/SiO₂ catalysts. Moreover, AuPd/SiO₂ with AuPd alloy structure exhibited better catalytic activity and selectivity than a core(Au)-shell(Pd) structure. Zhang et al. [3] synthesized AuPd/SiO₂ catalysts by electroless deposition with various surface coverage of Au on Pd and observed the formation of small ensembles of Pd sites at high Au surface coverage, which promoted the adsorption of acetylene as π -bonded species favoring hydrogenation to ethylene, whereas at low Au surface coverage larger contiguous Pd ensembles were formed resulting in ethane formation. The ethylene selectivity was also decreased due to the strong adsorption of acetylene as multi σ -bonded species [16]. Furthermore, alloying Pd with small Au nanoparticles (~3 nm) on a SiO₂ support with Pd/Au atomic ratios < 0.025 exhibited higher catalytic performance than the monometallic Pd or Au [12]. Pei et al. [12] proposed that Pd promoted acetylene conversion at lower reaction temperature, compared to Au, whereas the Au addition helped to isolate the Pd atoms and suppressed the hydrogenation of ethylene to ethane (improvement in selectivity). Additionally a weaker ethylene adsorption was observed for the AuPd/SiO₂ catalysts with Pd single-atom alloy structure in comparison to the monometallic Pd/SiO₂, thus leading to higher ethylene selectivity [12]. Zhang et al. [15] synthesized AuPd/TiO₂ catalyst (Au/Pd atomic ratio = 14) by deposition-precipitation of Au followed by impregnation with Pd. Large amount of surface Pd sites (both of isolated Pd atoms and contiguous Pd clusters) were formed, facilitating acetylene adsorption leading to the improvement of acetylene conversion.

Flame spray pyrolysis (FSP) technology has a great potential for rapid, flexible, and scalable synthesis of multi-component nanoparticles. The characteristics of such nanoparticles can be tuned by the FSP operating conditions such as precursor type [17, 18], concentration [19-21], flow rate [19, 21, 22], type of solvent [23, 24], dispersion gas type [19], dispersion gas flow rate [19, 21], and other process conditions [20, 21]. By varying these parameters, the combustion enthalpy change which affects the total net heating value of the spray flame. The metal precursor and solvent should be selected not only by their miscibility but also suitable combustion enthalpy for the FSP synthesis method.

The 2-nozzle FSP facilitates a better control of the mixing intensity of the individual components of the two flames [25]. Up to date, only a few catalyst systems have been reported using 2-nozzle FSP synthesis method (e.g., Al_2O_3 and $\text{Ce}_x\text{Zr}_{1-x}\text{O}_2$ supported Pt-Ba catalysts [26, 27] for NO_x storage, CoMo/ Al_2O_3 [25] hydrotreating catalysts, Ba- and K-promoted Rh/ Al_2O_3 [28] for CO_2 hydrogenation, and CO oxidation catalysts based on Pt- $\text{FeO}_x/\text{CeO}_2$ [29], $\text{MnO}_x/\text{Al}_2\text{O}_3$, and $\text{FeO}_x/\text{Al}_2\text{O}_3$ [30]). An important feature of the 2-nozzle FSP emerging from these previous studies is that the incorporation of the active phase into the oxide support could be prevented.

The 2-nozzle FSP allows designing multi-component nanoparticles by controlling the mixing of the individual components from the two flames. The present work reports the characteristics as well as the catalytic properties of the bimetallic AuPd/ TiO_2 made by 2-nozzle FSP with different noble metal mixing. The degree of AuPd alloy formation, the interaction between metal-metal and metal-support, and the location of Pd (or AuPd) on the TiO_2 could be varied significantly. The catalysts were characterized by N_2 physisorption, X-ray diffraction (XRD), CO chemisorption, scanning transmission electron microscopy (STEM), energy-dispersive X-ray spectroscopy (EDXS), and X-ray photoelectron

spectroscopy (XPS). Their catalytic performances were evaluated for low temperature (40 °C) gas-phase selective hydrogenation of acetylene in excess ethylene.

2. Experimental

2.1 Catalyst preparation

The bimetallic 1 wt.% Au-1 wt.% Pd/TiO₂ catalysts were prepared by 1- and 2-nozzle FSP using palladium (II) acetylacetonate, gold (III) chloride hydrate (Sigma-Aldrich), and titanium isopropoxide (Sigma-Aldrich) as precursors. For the conventional 1-nozzle FSP, all precursors were dissolved in xylene/acetonitrile (70/30 vol%) mixture solution of 0.5 M total metal (Au, Pd, Ti) concentration. This precursor solution was fed through the FSP nozzle by a syringe pump and dispersed with O₂ to form a fine spray of droplet. The precursor flow rate was 5 mL/min while the flow rate of O₂ dispersion was 5 L/min. The supporting premixed flame feed gases consisting of O₂ (2 L/min) and CH₄ (1 L/min) were provided through a ring around the nozzle dispersion O₂ outlet to ignite the spray resulting in a self-sustaining spray flame. The produced particles were collected on a glass fiber filter with the aid of a vacuum pump. With the 2-nozzle FSP and the specified liquid precursor solutions, four different AuPd/TiO₂ catalyst particle configurations were prepared differing in the separation of TiO₂, Pd and Au components. In the notation used here the catalysts produced with 2-nozzle FSP are labeled with + symbol: Each side of the + indicates which metals were produced in the same nozzle. As an example "TiO₂+AuPd" indicates that the Ti precursor was fed through one nozzle while the Au and Pd precursors were fed through the other nozzle. The production with 1- and 2-nozzles is schematically shown in **Fig. 1**.

Catalyst preparation with 2-nozzle FSP was similar to that with 1-nozzle FSP. For each nozzle, the liquid precursor solution was fed at 5 mL/min and dispersed with O₂ at 5 L/min forming a fine spray. The angle between the two nozzles was maintained at 160°, resulting in a meeting distance of the center of both nozzles equal to 32 cm.

For comparison of the catalytic performance, bimetallic AuPd/TiO₂ catalysts prepared by conventional methods and a commercial acetylene hydrogenation catalyst were also tested. The bimetallic 1 wt.% Au-1 wt.% Pd/TiO₂ catalysts were prepared by conventional co-impregnation (IMP) and deposition-precipitation (DP) methods according to the procedures described in Ref. [31]. The commercial acetylene hydrogenation catalyst was a bimetallic Pd-Ag/Al₂O₃ catalyst (Süd-Chemie).

2.2 Catalyst characterization

The XRD patterns were recorded from 20° to 70° by a Bruker AXS D8 Advance diffractometer (40 kV, 40mA, $\lambda = 0.154$ nm) with Cu K α radiation. The crystallite sizes were calculated by Topas 3 software with the Rietveld refinement. The phase composition of TiO₂ was calculated by [32]:

$$W_R = \left(\frac{1}{0.884 \left(\frac{A}{R} \right) + 1} \right) \times 100$$

where W_R is the mass fraction of rutile, A and R are the peak areas of anatase (101) and rutile (110), respectively. The number of 0.884 is the coefficient of scattering. The BET measurement was performed by nitrogen adsorption at 77 K using a Micromeritics Tristar instrument. The BET specific surface area (SSA) was measured by a 5-point nitrogen adsorption isotherm after degassing of the sample with N₂ at 200 °C for at least 1 h. The

actual metal loadings in the catalyst sample were analyzed by ICP-OES technique using a Horiba Jobin Yvon Activa spectrometer. The chemisorbed CO on the samples was measured by CO-pulse chemisorption using a Micromeritics Autochem II 2920 equipped with a thermal conductivity detector (TCD) and mass spectrometer (MS). Before chemisorption, the samples were reduced with 5% H₂/Ar at 150 °C for 2 h. The CO was injected to the reduced catalysts with 10 pulses at 40 °C or until the MS signal of effluent CO gas was constant. The HAADF (high angle annular dark-field) imaging and the EDX analysis of the nanoparticles within the samples was performed by an aberration-corrected STEM/SEM HD-2700CS HITACHI microscope operated in the STEM mode equipped with an SDD energy-dispersive X-ray spectrometer (EDX) and Genesis Spectrum (version 6.2) software from EDAX. The XPS was performed on a Kratos AMICUS X-ray photoelectron spectrometer using MgK_α as X-ray radiation. The C 1s line (binding energy at 285.0 eV) was specified as internal standard.

2.3 Catalytic reaction study

The selective hydrogenation of acetylene in excess ethylene was performed in a quartz reactor (inner tube diameter 4 mm) at 40 °C. Prior to the reaction, 50 mg of catalyst was reduced with H₂ (50 mL/min) at 150 °C for 2 h, and then cooled down to the reaction temperature at 40 °C under He (30 ml/min). A gaseous mixture containing 1.5% C₂H₂, 2% H₂ and the balance C₂H₄ was introduced into the reactor at a total flow rate of 100 mL/min. The reaction temperature was kept constant for 1 h. The gas mixture at the outlet of the reactor was analyzed by an on-line gas chromatograph equipped with a flame ionization detector (FID) and a HP-PLOT Q column 30 m length, 0.32 mm in diameter and 0.2 μm film thickness (Agilent Technologies).

The ethylene selectivity was calculated from the measured ethane formation [33]. As the hydrogenation of acetylene was investigated in the excess ethylene (96.5 vol%), a change in the ethylene concentration could not have been detected accurately enough. The acetylene conversion and ethylene selectivity are defined as follows [12, 33-35]:

$$\text{Acetylene conversion} = \frac{C_2H_2(in) - C_2H_2(out)}{C_2H_2(in)} \times 100\%$$

$$\text{Ethylene selectivity} = \left(1 - \frac{C_2H_6(out) - C_2H_6(in)}{C_2H_2(in) - C_2H_2(out)} \right) \times 100\%$$

Ethylene and ethane are assumed to be the only products for selective hydrogenation of acetylene, as no other GC signals were observed and due to the short contact time oligomerization was negligible [12, 36, 37]. $C_2H_6(in)$ represents the C_2H_6 impurity concentration in the C_2H_4 cylinder used.

3. Results and discussion

3.1 Catalyst characterization

With the 2-nozzle FSP system the mixing intensity of the noble metals and the support was controlled [26, 38, 39]. A schematic diagram showing the structural features of the AuPd/TiO₂ prepared by different routes using 1- and 2-nozzle FSP systems is shown in **Fig. 1**. These features emerged from the characterization results of the techniques used, including XRD, N₂ physisorption, CO chemisorption, XPS, and STEM-EDX. In **Fig. 2** the XRD patterns of all catalysts are shown. The major phase was anatase (TiO₂). The average TiO₂ crystallite size, BET surface area, and CO chemisorption results of the catalysts are summarized in **Table 1**. The average crystallite size of anatase was around 16 nm for

catalysts made by 2-nozzles and was similar to that prepared by the 1-nozzle (18 nm). An exception is "Pd/TiO₂+Au/TiO₂" with a TiO₂ crystallite size of 12 nm, which is attributed to the division in halves of the Ti concentrations fed to the individual nozzles (total Ti concentration fed to the flames was constant for all catalyst preparations). It has been shown previously that the precursor concentration defines the growth rate of the particles [20]. The smaller crystallite size of the anatase TiO₂ of "Pd/TiO₂+Au/TiO₂" is in agreement with the higher BET specific surface area (152 m²/g corresponding to a d_{BET} of 10 nm). All other samples had significantly lower surface areas in the range of 99-106 m²/g (d_{BET} of 15 nm). The actual Pd and Au metal loadings in the catalyst samples were analyzed by ICP-OES technique as shown in **Table 1**. According to ICP results, it could confirm that almost of Pd and Au metals were retained within the catalyst matrix.

The amount of CO adsorbed on the various catalysts listed in **Table 1** was used to calculate the Pd dispersion. The "Au/TiO₂+Pd" catalyst showed the highest dispersion of 23%. Separating the Pd precursor into the 2nd nozzle FSP prevented the coverage of Pd particles by Ti-O species, resulting in higher fraction of active Pd surface sites accessible for CO chemisorption. Among the AuPd/TiO₂ catalysts, the 1-nozzle FSP-AuPd/TiO₂ and the "TiO₂+AuPd" showed relatively low Pd dispersion probably due to formation of AuPd bimetallic particles with Au enriched on the surface due to lower surface free energy of Au compared to Pd [40]. In addition, the synthesis of AuPd/TiO₂ using 1-nozzle FSP can lead to the formation of Ti-O species covering the AuPd alloy particles. As a result, CO could not adsorb on Pd sites and hence a low CO uptake and low Pd dispersion was observed. This is in line with the previous observation made by Mekasuwandumrong et al. [41], who reported that the simultaneous condensation of Pd and TiO₂ leads to partial coverage of Pd by TiO₂. The calculated Pd dispersion of the "Pd/TiO₂+Au" and "Pd/TiO₂+Au/TiO₂" was 17 and 20%,

respectively, with a relatively high Pd dispersion, since Pd was sprayed separately from Au and less (or even no) AuPd alloys could be formed.

The binding energy of the Pd 3d and Au 4f and the surface atomic compositions of the metal species on the catalyst samples are presented in **Table 2** and **3**, respectively. The typical binding energy of Pd 3d for Pd metal was reported to be in the range of 335.0-335.4 eV [42]. The XPS peaks for Pd 3d were shifted towards lower binding energy upon AuPd alloy formation [43, 44] whereas shifting towards higher binding energy can be assigned to electron-deficient Pd such as Pd oxide [45]. According to **Table 2**, the XPS Pd 3d spectra for all samples were fitted with FWHM < 2 into 3 types indicating 3 components presented as Pd in AuPd alloy, Pd metal, and Pd oxide. The binding energy of the Pd 3d peaks in AuPd alloy for the "TiO₂+AuPd" was lowest; in addition, the percentage of Pd forming AuPd alloy was highest. It is suggested that the well-mixing between Au and Pd precursors in the nozzle where only Pd and Au precursors were fed promoted the degree of AuPd alloy formation. Compared to the "TiO₂+AuPd", the "AuPd/TiO₂" prepared by 1-nozzle FSP showed higher binding energy of Pd 3d indicating weaker interaction between Au and Pd in bimetallic AuPd particles and lower fraction of Pd being involved in alloy structure due to the presence of Ti precursor together with Au and Pd precursors in the same nozzle. For the other catalysts prepared by 2-nozzle FSP, the observed Pd forming bimetallic AuPd alloy structure showed higher binding energy and lower fraction of Pd involved in AuPd alloy structure. These results indicate that the separation of the noble metal precursors by feeding to different nozzles leads to weak interaction between Au and Pd. In other words, their late mixing in the flame strongly suppresses the formation of bimetallic AuPd structure with strong interaction between Pd and Au. Furthermore, the fraction of Pd oxide was significantly higher for the catalysts prepared by feeding Pd and Ti precursors together, as exemplified by "Pd/TiO₂+Au". The XPS Au 4f spectra for all the samples were fitted with one component

for Au species (FWHM < 2 eV). The surface atomic ratio listed in **Table 3** indicates that the sample "AuPd/TiO₂" made by 1-nozzle FSP has the lowest surface atomic composition of both Au and Pd, proposing partial coverage of the metal particles with Ti-O species. The "TiO₂+AuPd" catalyst showed the highest Au and Pd atomic percentages, indicating the presence of both Au and Pd on the catalyst surface. For the other particle configurations, the separation of the flames fed with Au or Pd precursors from the one fed with Ti support precursor resulted in poor mixing between noble metal and Ti precursors, leading to lower coverage of the noble metals with Ti-O species.

The HAADF (Z-contrast) images of the bimetallic AuPd/TiO₂ catalysts and selected (typical) EDX spectra of individual AuPd nanoparticles within each sample prepared by the 2-nozzle FSP are shown in **Fig. 3(a) and (b)** respectively. In the HAADF images the bimetallic nanoparticles appear as bright spots since the collected intensity is directly related to the atomic number Z, the dependency being roughly proportional to Z² [46, 47]. The STEM-EDX analysis performed on several individual nanoparticles in each sample confirmed the presence of both Au and Pd metals within each of them. This indicates the bimetallic nature of the nanoparticles. Although all the catalysts showed the presence of both Au and Pd metals in each analyzed nanoparticle, the fractions of Au and Pd within the nanoparticles were different for each catalyst prepared by the 2-nozzle FSP. The "TiO₂+AuPd" catalyst showed a higher fraction of Pd (higher Pd/Au ratio) compared to the others. Furthermore, in the "Au/TiO₂+Pd" catalyst, small Pd particles dispersed on the TiO₂ support were also detected in addition to the bimetallic ones. The former can be clearly identified by EDX but also directly in the corresponding image HAADF in **Fig. 3(a)** since they are much smaller and as such a much weaker contrast, due to smaller number of atoms with lower Z, than the bimetallic ones.

3.2 Selective hydrogenation of acetylene over the AuPd/TiO₂ catalysts

The performances of the AuPd/TiO₂ catalysts prepared by 1- and 2-nozzle FSP were examined in the selective hydrogenation of acetylene at 40 °C and the results are shown in **Fig. 4**. For the FSP-made catalysts, the conversion of acetylene followed the order: "TiO₂+AuPd" > "Au/TiO₂+Pd" > "AuPd/TiO₂ 1-nozzle" > "Pd/TiO₂+Au" ≈ "Pd/TiO₂+Au/TiO₂". Despite its lower CO uptake and lower Pd dispersion, the "TiO₂+AuPd" from the 2-nozzle FSP exhibited the highest acetylene conversion under the reaction conditions used. The activity of the TiO₂ supported AuPd bimetallic catalysts also did not depend much on the physical properties the TiO₂ but rather affected by the fraction and the location of the bimetallic alloy particles. The results in this study suggest that the formation of bimetallic AuPd particles enhanced the rate for acetylene hydrogenation. It has previously been found that the presence of AuPd alloy also greatly enhanced the hydrogenation rate of 1-heptyne under mild reaction conditions [31, 48]. Moreover, the location of Pd or AuPd seems to have a strong effect on the catalyst activity in the acetylene hydrogenation reaction. The hydrogenation activity of the "TiO₂+AuPd" and "Au/TiO₂+Pd", in which most of the Pd (or AuPd) particles were deposited on the surface of the TiO₂ support (less coverage by Ti-O) was higher than those where Pd and Ti precursor were mixed in a single flame (i.e., "AuPd/TiO₂ 1-nozzle", "Pd/TiO₂+Au", and "Pd/TiO₂+Au/TiO₂"). In addition, the separation of Pd and Au precursors into individual nozzles might result in weak interaction between Pd and Au and partial coverage of the noble metal particles by the TiO₂ support and consequently the lowest acetylene conversion was obtained. Nevertheless, the selectivity to ethylene was > 95% for all the flame-made catalysts. As acetylene adsorption is stronger than that of ethylene, the latter may be desorbed before its complete hydrogenation to ethane [49]. The selectivity to ethylene has previously been shown to be significantly improved by adding Au as the second metal to the Pd-based catalysts [3, 12, 13]. For the AuPd/SiO₂ catalysts

prepared by the electroless deposition of Au on Pd/SiO₂, ethylene selectivity was improved up to 75% compared to the monometallic Pd/SiO₂ (55%) [3]. The Pd single atom alloy structure in the AuPd/SiO₂ catalysts also exhibited higher ethylene selectivity (~85%) compared to the monometallic Pd (50%) due to the weaker ethylene adsorption [12].

For comparison, the commercial acetylene hydrogenation catalyst and corresponding AuPd/TiO₂ catalysts synthesized by conventional co-impregnation (IMP) and deposition-precipitation (DP) were tested under similar reaction conditions. The physicochemical and catalytic properties of the IMP- and DP-AuPd/TiO₂ catalysts compared to the "AuPd/TiO₂ 1-nozzle" have been reported in a previous study for 1-heptyne hydrogenation [31]. The results of the comparative catalytic tests summarized in Fig. 4 show that the FSP-synthesized AuPd/TiO₂ in this study exhibited superior catalytic performances compared to the commercial catalyst (C₂H₂ conversion 17% and C₂H₄ selectivity 90%). The IMP- and DP-AuPd/TiO₂ catalysts also showed higher conversion of C₂H₂ than the commercial catalyst but their selectivities to ethylene were lowest among the various catalysts studied. Unlike as with the FSP-made AuPd/TiO₂, non-uniform distribution of bimetallic AuPd particles was observed on the catalysts prepared by DP or IMP, resulting in poor catalytic performances [31]. As shown in this study, the properties of the 1-nozzle FSP bimetallic AuPd/TiO₂ can be further improved by using the 2-nozzle FSP, which also offers interesting possibilities for large scale production of catalysts with unique and tailored properties for particular applications.

4. Conclusions

Two-nozzle FSP facilitated the synthesis of various configurations of TiO₂-supported noble metal nanoparticles. Feeding all precursor components to a single nozzle results in

titania-supported bimetallic as well monometallic noble metal particles. Proper use of a 2-nozzle system leads to significantly higher variability in the achievable particle configurations. Bimetallic nanoparticle formation can be minimized by feeding the noble metal precursors separately to the two nozzles, while co-feeding of the noble metal precursors affords predominantly bimetallic particles. Also the support TiO_2 could either be produced by co-feeding either one or both noble metal precursors. For the selective hydrogenation of acetylene in excess ethylene, highest conversion was achieved at 40°C for catalysts produced by feeding Au and Pd precursors to the same nozzle and the Ti precursor to the other one ("TiO₂+AuPd"), indicating that maximizing the fraction of bimetallic alloy particles is beneficial for the selective hydrogenation of acetylene. The enhanced hydrogenation activity at high selectivity to ethylene (>95%) is attributed to the presence of bimetallic AuPd particles, as indicated by XPS and STEM-EDX results. The catalysts made by co-feeding of one or both of the noble metals together with Ti ("Pd/TiO₂+Au", "Pd/TiO₂+Au/TiO₂", and "AuPd/TiO₂ 1-nozzle") led to partial coverage of Pd by Ti-O species, as indicated by CO chemisorption measurements, and consequently lower acetylene conversions were obtained on these three catalysts.

Acknowledgements

This research is supported by Ratchadaphiseksomphot Endowment Fund, Chulalongkorn University for the Postdoctoral Fellowship (B.P.) and the International Research Integration: Chula Research Scholar. We thank Dr. Frank Krumeich (ETH) for STEM/EDXS investigation and the Electron Microscopy Center of ETH Zurich (EMEZ) for providing the necessary infrastructure. The research leading to these results has also received partial funding from the Thailand Research Fund (BRG5780010) and the European Research

Council under the European Union's Seventh Framework Program (FP7/2007-2013) / ERC
grant agreement n° 247283.

References

- [1] N.A. Khan, S. Shaikhutdinov, H.-J. Freund, Acetylene and Ethylene Hydrogenation on Alumina Supported Pd-Ag Model Catalysts, *Catal. Lett.*, 108 (2006) 159-164.
- [2] A. Yildirim, H. Koc, E. Deligoz, First-principles study of the structural, elastic, electronic, optical, and vibrational properties of intermetallic Pd₂Ga, *Chinese Physics B*, 21 (2012) 037101.
- [3] Y. Zhang, W. Diao, C.T. Williams, J.R. Monnier, Selective hydrogenation of acetylene in excess ethylene using Ag- and Au-Pd/SiO₂ bimetallic catalysts prepared by electroless deposition, *Appl. Catal. A: Gen.*, 469 (2014) 419-426.
- [4] W.-J. Kim, S.H. Moon, Modified Pd catalysts for the selective hydrogenation of acetylene, *Catal. Today*, 185 (2012) 2-16.
- [5] S. Lee, Partial Catalytic Hydrogenation of Acetylene in Ethylene Production, Johor, Malaysia: KLM Technology Group. Retrieved from [http://www.klmtechgroup.com/PDF/Articles/acetylene converter. pdf](http://www.klmtechgroup.com/PDF/Articles/acetylene%20converter.pdf), 2004.
- [6] H. Zea, K. Lester, A.K. Datye, E. Rightor, R. Gulotty, W. Waterman, M. Smith, The influence of Pd-Ag catalyst restructuring on the activation energy for ethylene hydrogenation in ethylene-acetylene mixtures, *Appl. Catal. A: Gen.*, 282 (2005) 237-245.
- [7] S. Leviness, V. Nair, A.H. Weiss, Z. Schay, L. Guzzi, Acetylene hydrogenation selectivity control on PdCu/Al₂O₃ catalysts, *J. Mol. Catal.*, 25 (1984) 131-140.
- [8] S. Chinayon, O. Mekasuwandumrong, P. Praserthdam, J. Panpranot, Selective hydrogenation of acetylene over Pd catalysts supported on nanocrystalline α -Al₂O₃ and Zn-modified α -Al₂O₃, *Catal. Commun.*, 9 (2008) 2297-2302.
- [9] S. Komhom, O. Mekasuwandumrong, P. Praserthdam, J. Panpranot, Improvement of Pd/Al₂O₃ catalyst performance in selective acetylene hydrogenation using mixed phases Al₂O₃ support, *Catal. Commun.*, 10 (2008) 86-91.
- [10] S.K. Kim, C. Kim, J.H. Lee, J. Kim, H. Lee, S.H. Moon, Performance of shape-controlled Pd nanoparticles in the selective hydrogenation of acetylene, *J. Catal.*, 306 (2013) 146-154.
- [11] T.V. Choudhary, C. Sivadinarayana, A.K. Datye, D. Kumar, D.W. Goodman, Acetylene Hydrogenation on Au-Based Catalysts, *Catal. Lett.*, 86 (2003) 1-8.
- [12] G.X. Pei, X.Y. Liu, A. Wang, L. Li, Y. Huang, T. Zhang, J.W. Lee, B.W.L. Jang, C.-Y. Mou, Promotional effect of Pd single atoms on Au nanoparticles supported on silica for the selective hydrogenation of acetylene in excess ethylene, *New J. Chem.*, 38 (2014) 2043-2051.
- [13] A. Sárkány, A. Horváth, A. Beck, Hydrogenation of acetylene over low loaded Pd and Pd-Au/SiO₂ catalysts, *Appl. Catal. A: Gen.*, 229 (2002) 117-125.
- [14] A. Sárkány, O. Geszti, G. Sáfrán, Preparation of Pd_{shell}-Au_{core}/SiO₂ catalyst and catalytic activity for acetylene hydrogenation, *Appl. Catal. A: Gen.*, 350 (2008) 157-163.
- [15] S. Zhang, C.-Y. Chen, B.W.L. Jang, A.-M. Zhu, Radio-frequency H₂ plasma treatment of AuPd/TiO₂ catalyst for selective hydrogenation of acetylene in excess ethylene, *Catal. Today*, 256, Part 1 (2015) 161-169.
- [16] S. Riyapan, Y. Zhang, A. Wongkaew, B. Pongthawornsakun, J.R. Monnier, J. Panpranot, Preparation of improved Ag-Pd/TiO₂ catalysts using the combined strong electrostatic adsorption and electroless deposition methods for the selective hydrogenation of acetylene, *Catal. Sci. Technol.*, 6 (2016) 5608-5617.
- [17] H.K. Kammler, L. Mädler, S.E. Pratsinis, Flame Synthesis of Nanoparticles, *Chem. Eng. Technol.*, 24 (2001) 583-596.
- [18] J.S. Lee, A. Khanna, M. Oh, M.B. Ranade, R.K. Singh, Synthesis and Characterization of Zn₂SiO₄:Mn²⁺ Nanophosphors Prepared from Different Zn Source in Liquid Precursor by Flame Spray Pyrolysis, *ECS Transactions*, 25 (2009) 107-112.

- [19] R. Mueller, L. Mädler, S.E. Pratsinis, Nanoparticle synthesis at high production rates by flame spray pyrolysis, *Chem. Eng. Sci.*, 58 (2003) 1969-1976.
- [20] H. Chang, S.J. Kim, H.D. Jang, J.W. Choi, Synthetic routes for titania nanoparticles in the flame spray pyrolysis, *Colloids Surf. A*, 313–314 (2008) 282-287.
- [21] G.L. Chiarello, I. Rossetti, L. Forni, Flame-spray pyrolysis preparation of perovskites for methane catalytic combustion, *J. Catal.*, 236 (2005) 251-261.
- [22] T. Tani, L. Mädler, S. Pratsinis, Homogeneous ZnO Nanoparticles by Flame Spray Pyrolysis, *J. Nanopart. Res.*, 4 (2002) 337-343.
- [23] L. Mädler, S.E. Pratsinis, Bismuth Oxide Nanoparticles by Flame Spray Pyrolysis, *J. Am. Ceram. Soc.*, 85 (2002) 1713-1718.
- [24] X. Qin, Y. Ju, S. Bernhard, N. Yao, Synthesis of $Y_2O_3:Eu$ Phosphor Nanoparticles by Flame Spray Pyrolysis, *NSTI-Nanotech 2005*, 2005, pp. 9-12.
- [25] M. Høj, D.K. Pham, M. Brorson, L. Mädler, A.D. Jensen, J.-D. Grunwaldt, Two-Nozzle Flame Spray Pyrolysis (FSP) Synthesis of $CoMo/Al_2O_3$ Hydrotreating Catalysts, *Catal. Lett.*, 143 (2013) 386-394.
- [26] R. Strobel, L. Mädler, M. Piacentini, M. Maciejewski, A. Baiker, S.E. Pratsinis, Two-Nozzle Flame Synthesis of $Pt/Ba/Al_2O_3$ for NO_x Storage, *Chem. Mater.*, 18 (2006) 2532-2537.
- [27] R. Strobel, F. Krumeich, S.E. Pratsinis, A. Baiker, Flame-derived $Pt/Ba/Ce_xZr_{1-x}O_2$: Influence of support on thermal deterioration and behavior as NO_x storage-reduction catalysts, *J. Catal.*, 243 (2006) 229-238.
- [28] R. Büchel, A. Baiker, S.E. Pratsinis, Effect of Ba and K addition and controlled spatial deposition of Rh in Rh/Al_2O_3 catalysts for CO_2 hydrogenation, *Appl. Catal. A: Gen.*, 477 (2014) 93-101.
- [29] J.A.H. Dreyer, H.K. Grossmann, J. Chen, T. Grieb, B.B. Gong, P.H.L. Sit, L. Mädler, W.Y. Teoh, Preferential oxidation of carbon monoxide over $Pt-FeO_x/CeO_2$ synthesized by two-nozzle flame spray pyrolysis, *J. Catal.*, 329 (2015) 248-261.
- [30] M. Tepluchin, D.K. Pham, M. Casapu, L. Mädler, S. Kureti, J.-D. Grunwaldt, Influence of single- and double-flame spray pyrolysis on the structure of $MnO_x/\gamma-Al_2O_3$ and $FeO_x/\gamma-Al_2O_3$ catalysts and their behaviour in CO removal under lean exhaust gas conditions, *Catal. Sci. Technol.*, 5 (2015) 455-464.
- [31] B. Pongthawornsakun, S.-i. Fujita, M. Arai, O. Mekasuwandumrong, J. Panpranot, Mono- and bi-metallic $Au-Pd/TiO_2$ catalysts synthesized by one-step flame spray pyrolysis for liquid-phase hydrogenation of 1-heptyne, *Appl. Catal. A: Gen.*, 467 (2013) 132-141.
- [32] A.A. Gribb, J.F. Banfield, Particle size effects on transformation kinetics and phase stability in nanocrystalline TiO_2 , *Am. mineral.*, 82 (1997) 717-728.
- [33] X. Liu, Y. Li, J.W. Lee, C.-Y. Hong, C.-Y. Mou, B.W.L. Jang, Selective hydrogenation of acetylene in excess ethylene over SiO_2 supported $Au-Ag$ bimetallic catalyst, *Appl. Catal. A: Gen.*, 439–440 (2012) 8-14.
- [34] X. Liu, C.-Y. Mou, S. Lee, Y. Li, J. Secrest, B.W.L. Jang, Room temperature O_2 plasma treatment of SiO_2 supported Au catalysts for selective hydrogenation of acetylene in the presence of large excess of ethylene, *J. Catal.*, 285 (2012) 152-159.
- [35] D. Duca, F. Frusteri, A. Parmaliana, G. Deganello, Selective hydrogenation of acetylene in ethylene feedstocks on Pd catalysts, *Appl. Catal. A: Gen.*, 146 (1996) 269-284.
- [36] G.X. Pei, X.Y. Liu, A. Wang, A.F. Lee, M.A. Isaacs, L. Li, X. Pan, X. Yang, X. Wang, Z. Tai, K. Wilson, T. Zhang, Ag Alloyed Pd Single-Atom Catalysts for Efficient Selective Hydrogenation of Acetylene to Ethylene in Excess Ethylene, *ACS Catalysis*, 5 (2015) 3717-3725.

- [37] C. Moreno-Marrodan, F. Liguori, P. Barbaro, Continuous-flow processes for the catalytic partial hydrogenation reaction of alkynes, *Beilstein Journal of Organic Chemistry*, 13 (2017) 734-754.
- [38] R. Büchel, R. Strobel, S.E. Pratsinis, A. Baiker, Two-nozzle flame synthesis of Pt/Ba/Al₂O₃ for NO_x storage NSTI-Nanotech 2008, 2008, pp. 669-671.
- [39] Z. Wang, S. Pokhrel, M. Chen, M. Hunger, L. Mädler, J. Huang, Palladium-doped silica–alumina catalysts obtained from double-flame FSP for chemoselective hydrogenation of the model aromatic ketone acetophenone, *J. Catal.*, 302 (2013) 10-19.
- [40] R. Sharpe, J. Counsell, M. Bowker, Pd segregation to the surface of Au on Pd(111) and on Pd/TiO₂(110), *Surface Science*, 656 (2017) 60-65.
- [41] O. Mekasuwandumrong, S. Phothakwanpracha, B. Jongsomjit, A. Shotipruk, J. Panpranot, Liquid-Phase Selective Hydrogenation of 1-Heptyne over Pd/TiO₂ Catalyst Synthesized by One-Step Flame Spray Pyrolysis, *Catal. Lett.*, 136 (2010) 164-170.
- [42] M. Jin, J.-N. Park, J.K. Shon, J.H. Kim, Z. Li, Y.-K. Park, J.M. Kim, Low temperature CO oxidation over Pd catalysts supported on highly ordered mesoporous metal oxides, *Catal. Today*, 185 (2012) 183-190.
- [43] Y.S. Lee, Y. Jeon, Y.D. Chung, K.Y. Lim, C.N. Whang, S.J. Oh, Charge redistribution and electronic behavior in Pd-Au alloys, *J. Korean Phys. Soc.*, 37 (2000) 451-455.
- [44] Y. Sohn, D. Pradhan, K.T. Leung, Electrochemical Pd nanodeposits on a Au nanoisland template supported on Si(100): Formation of Pd-Au alloy and interfacial electronic structures, *ACS Nano*, 4 (2010) 5111-5120.
- [45] R.N. Lamb, B. Ngamsom, D.L. Trimm, B. Gong, P.L. Silveston, P. Praserttham, Surface characterisation of Pd–Ag/Al₂O₃ catalysts for acetylene hydrogenation using an improved XPS procedure, *Appl. Catal. A: Gen.*, 268 (2004) 43-50.
- [46] S.J. Pennycook, Z-contrast stem for materials science, *Ultramicroscopy*, 30 (1989) 58-69.
- [47] M.M.J. Treacy, Z dependence of electron scattering by single atoms into annular dark-field detectors, *Microscopy and Microanalysis*, 17 (2011) 847-858.
- [48] B. Pongthawornsakun, O. Mekasuwandumrong, S. Prakash, E. Ehret, F.J.C. Santos Aires, J. Panpranot, Effect of reduction temperature on the characteristics and catalytic properties of TiO₂ supported AuPd alloy particles prepared by one-step flame spray pyrolysis in the selective hydrogenation of 1-heptyne, *Appl. Catal. A: Gen.*, 506 (2015) 278-287.
- [49] C.L. Gordon, L.L. Lobban, R.G. Mallinson, Selective hydrogenation of acetylene to ethylene during the conversion of methane in a catalytic dc plasma reactor, in: J.J.S. E. Iglesia, T.H. Fleisch (Eds.) *Studies in Surface Science and Catalysis*, Elsevier 2001, pp. 271-276.

Figure captions

Figure 1. Schematic of the 1-nozzle and 2-nozzle FSP for the preparation of AuPd supported on TiO₂.

Figure 2. XRD patterns of AuPd/TiO₂ catalysts prepared by different routes (a) AuPd/TiO₂ 1-nozzle, (b) Pd/TiO₂+Au, (c) Au/TiO₂+Pd, (d) TiO₂+AuPd (e) Pd/TiO₂+Au/TiO₂.

Figure 3. (a) STEM-HAADF (Z-contrast) images and (b) STEM-EDX of individual bimetallic AuPd/TiO₂ catalysts.

Figure 4. Catalytic performance at 40 °C of AuPd/TiO₂ catalysts prepared by different routes in selective acetylene hydrogenation in excess ethylene (◆ : AuPd/TiO₂ prepared by one nozzle FSP, ■ : TiO₂+AuPd, ▲ : Au/TiO₂+Pd, × : Pd/TiO₂+Au, ✱ : Pd/TiO₂+Au/TiO₂, ● : commercial PdAg/TiO₂ catalyst, + : AuPd/TiO₂ prepared by co-impregnation [31], - : AuPd/TiO₂ prepared by co-deposition precipitation [31]).

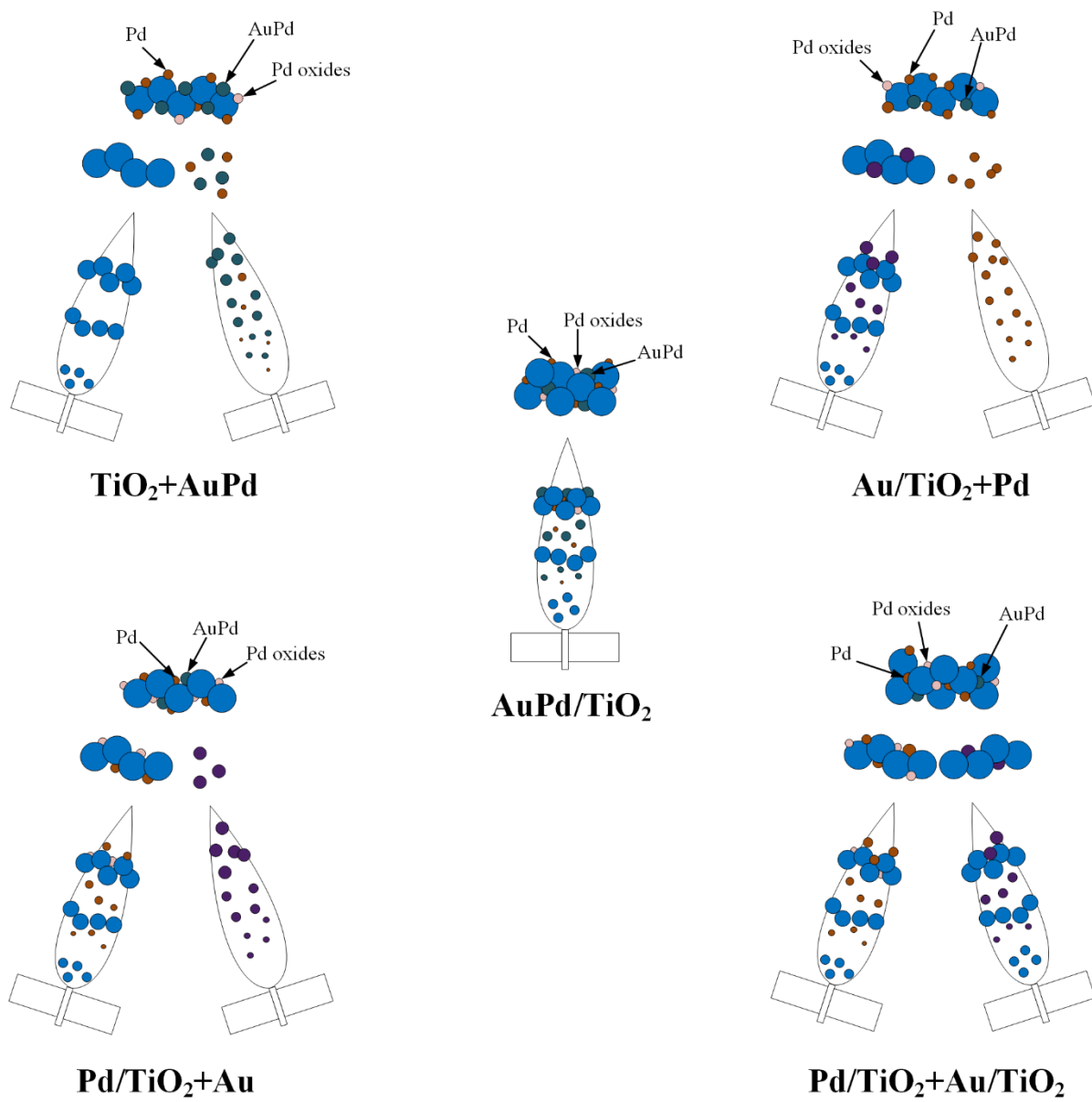


Figure 1

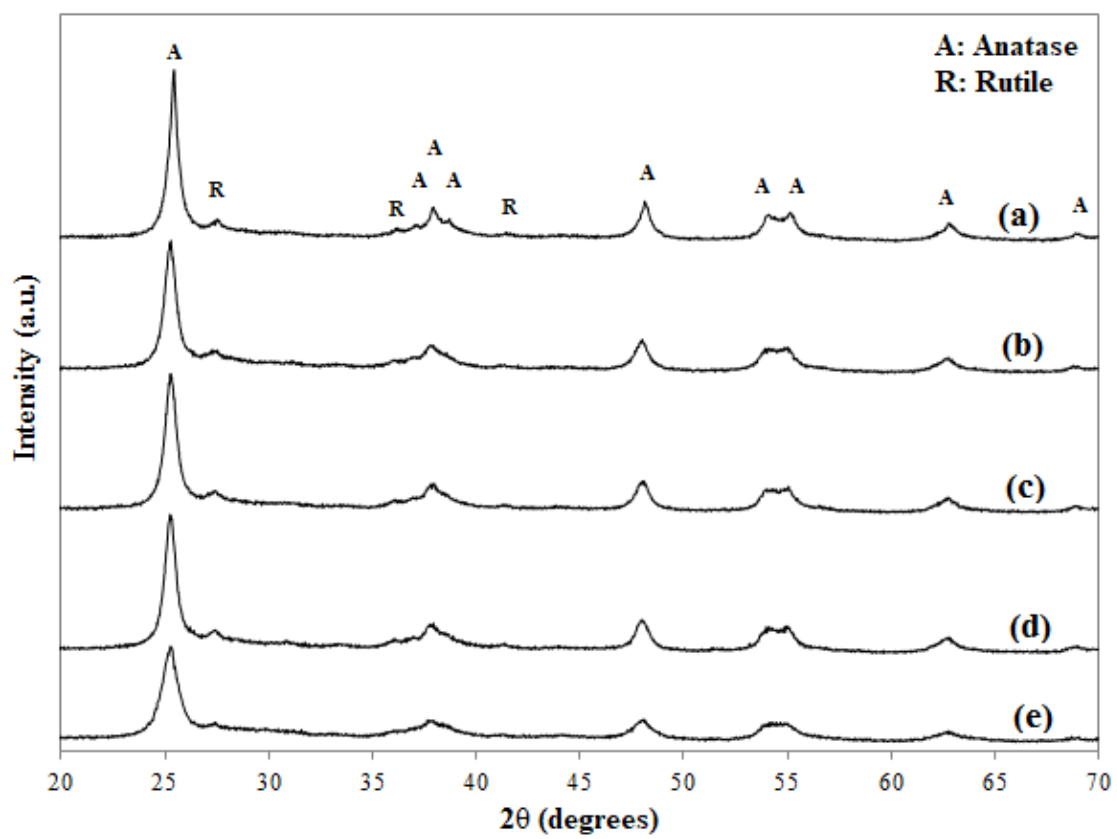


Figure 2

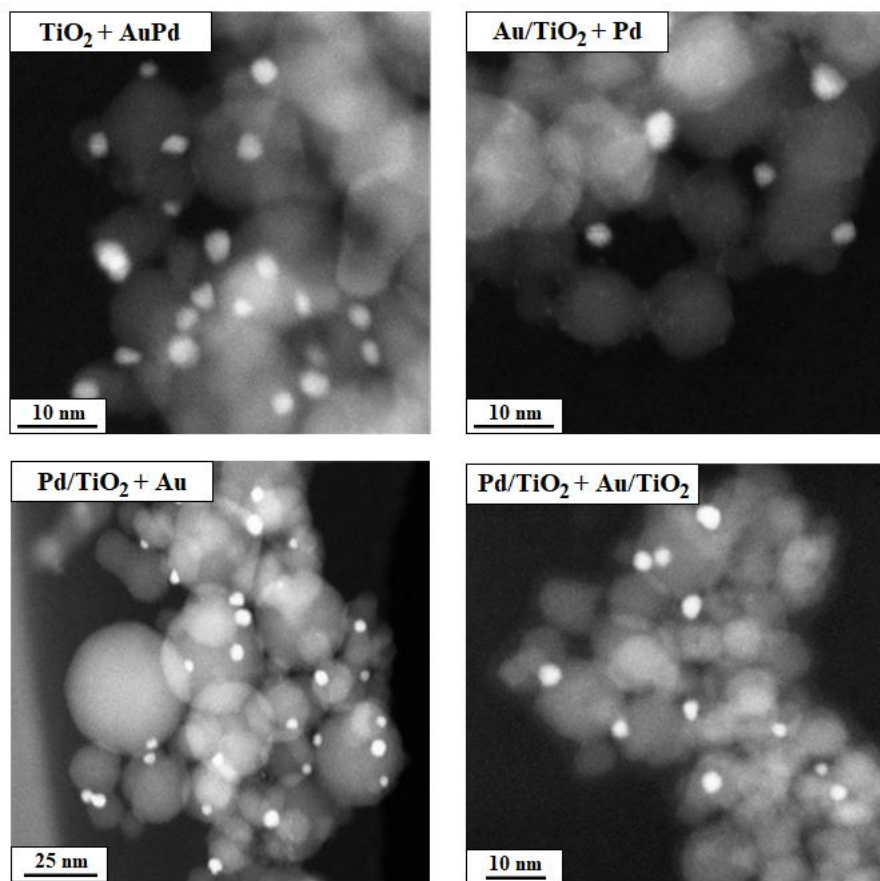


Figure 3(a)

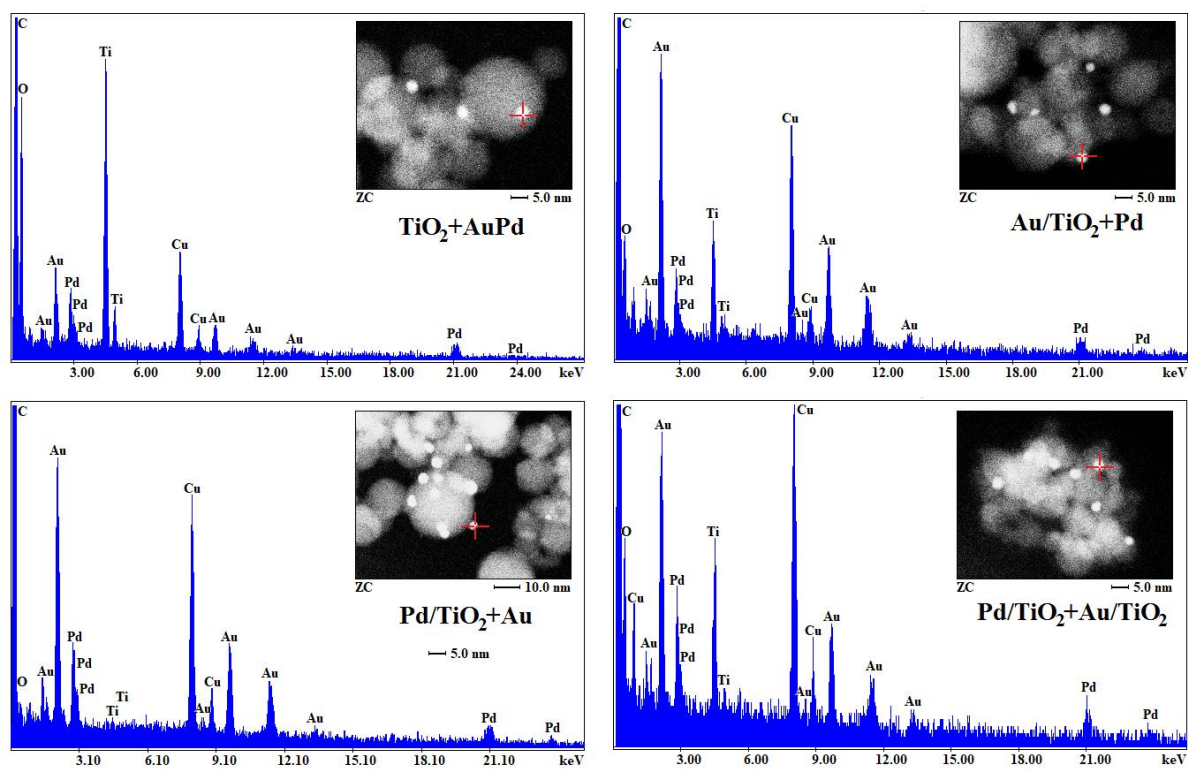


Figure 3(b)

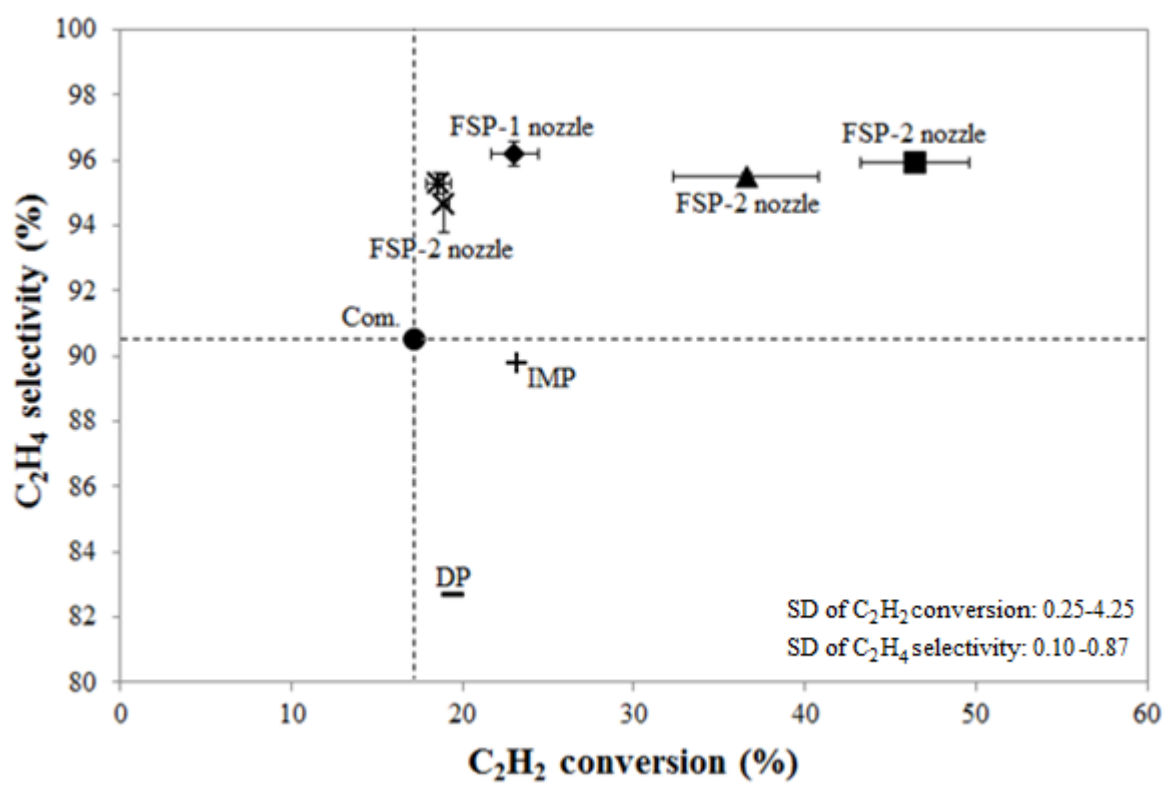


Figure 4

Table 1. Characteristics of the bimetallic AuPd/TiO₂ catalysts prepared by 1- and 2-nozzle

FSP

Catalysts	TiO ₂ crystallite size (nm)	BET surface area (m ² /g)	Metal loadings		CO uptake (μmole CO/g _{cat.})	Pd dispersion ^a (%)
			Pd (wt.%)	Au (wt.%)		
TiO ₂ + AuPd	17	104	0.94	0.82	9.3	13
Au/TiO ₂ + Pd	16	104	0.91	0.83	19.1	26
Pd/TiO ₂ + Au	16	99	0.89	0.87	13.8	19
Pd/TiO ₂ + Au/TiO ₂	12	152	0.90	0.88	16.3	22
AuPd/TiO ₂ 1-nozzle FSP	18	106	0.92	0.88	7.9	11
IMP-AuPd/TiO ₂ ^b	25	60	1.00	1.12	32.2	38
DP-AuPd/TiO ₂ ^b	28	65	0.98	0.61	28.6	34
Commercial catalyst PdAg/Al ₂ O ₃	n.d.	35	0.03	0.18	0.5	19

^aPd dispersion has been estimated from the actual metal loading and CO uptake measurements assuming a stoichiometric factor CO:Pd = 1:1

^bResults as cited in [31]

Table 2. Binding energy of Pd 3d and Au 4f of the bimetallic AuPd/TiO₂ catalysts prepared by 1- and 2-nozzle FSP

Catalyst	Pd alloy			Pd metal			Pd oxide			Au 4f		
	B.E. (eV)	FWHM	Area (%)									
TiO ₂ +AuPd	333.30	2.00	28	335.20	1.99	51	336.81	1.77	21	83.00	1.56	100
Au/TiO ₂ +Pd	334.16	1.88	21	335.20	2.00	56	337.21	1.88	23	82.65	1.47	100
Pd/TiO ₂ +Au	334.04	1.94	20	335.35	1.98	40	336.97	2.00	40	82.62	1.40	100
Pd/TiO ₂ +Au/TiO ₂	333.90	1.66	22	353.30	2.00	48	336.91	2.00	30	82.96	1.69	100
AuPd/TiO ₂ 1-nozzle	333.52	2.00	25	335.05	1.86	46	336.37	2.00	29	83.02	1.46	100

Table 3. Surface atomic composition of the bimetallic AuPd/TiO₂ catalysts prepared by 1- and 2-nozzle FSP

Catalysts	Atomic concentration		Atomic ratio		
	Pd (%)	Au (%)	Pd/Ti	Au/Ti	(Pd+Au)/Ti
	TiO ₂ + AuPd	0.501	0.165	0.023	0.008
Au/TiO ₂ + Pd	0.280	0.106	0.015	0.006	0.021
Pd/TiO ₂ + Au	0.249	0.139	0.013	0.008	0.021
Pd/TiO ₂ + Au/TiO ₂	0.259	0.127	0.012	0.006	0.019
AuPd/TiO ₂ 1-nozzle	0.225	0.085	0.012	0.004	0.016